

Integral Equation Theory of Polymer Melts: Density Fluctuations, Static Structure Factor, and Comparison with Incompressible and Continuum Limit Models^{†,‡}

Kenneth S. Schweizer* and John G. Curro

Sandia National Laboratories, Albuquerque, New Mexico 87185.

Received November 20, 1987; Revised Manuscript Received April 4, 1988

ABSTRACT: A detailed numerical study, utilizing our RISM integral equation theory, of the static structure factor and isothermal compressibility of athermal polymer melts composed of nonoverlapping freely jointed chains is reported. Trends associated with variable density, degree of polymerization, and intramolecular details are established. At small wave vectors a crossover in the behavior of the structure factor from semidilute-like Lorentzian decay to simple liquid behavior is found with increasing (decreasing) melt density (molecular weight). Comparison of the integral equation theory predictions for the intermolecular pair correlation function with those of a simple incompressible model and an analytical continuum limit model is carried out. The range of validity and limitations of these simplified descriptions for both the short-range order and the correlation hole are determined. Local intermolecular correlations out to three or four monomer diameters are poorly represented by the simple theories even at high densities and molecular weights. On the other hand, the long-range correlation hole structure is well described by the incompressible model and displays a large degree of universality.

I. Density Fluctuations and the Static Structure Factor

A. Basic Features. The static structure factor is the Fourier transform of the total density fluctuation correlation function and is defined as

$$\hat{S}(k) = N^{-1} \sum_{\alpha, \gamma=1}^N \hat{\omega}_{\alpha\gamma}(k) + \rho \hat{h}_{\alpha\gamma}(k) \quad (1a)$$

$$\hat{S}(k) = \hat{\omega}(k) + \rho_m \hat{h}(k) \quad (1b)$$

$$\hat{S}(k) = \hat{\omega}(k)[1 - \rho_m \hat{\omega}(k) \hat{C}(k)]^{-1} \quad (1c)$$

where eq 1c follows from employing the Fourier transforms of eq 4 of paper 1 (a monomer-independent scattering form factor is assumed). System specificity enters directly via the intramolecular structure factor, $\hat{\omega}(k)$, and also via the direct correlation function, $\hat{C}(k)$, which itself is a functional of $\hat{\omega}(k)$ through the RISM integral equation. The Fourier transform of the direct correlation function normalized by its zero wave vector limit is plotted in Figure 1 for several packing fractions, degrees of polymerization, and intramolecular models. At relatively small wave vectors, $k\sigma \lesssim 1$, $\hat{C}(k)$ is well described in all cases by the quadratic form:

$$\hat{C}(k) \simeq \hat{C}(0) + \frac{1}{2} k^2 \hat{C}''(0), \quad k\sigma \leq 1 \quad (2)$$

At larger wave vectors, $\hat{C}(k)$ displays some system specificity but retains the same qualitative shape. Both the rate of initial decay of $\hat{C}(k)$ and the depth of the local minimum increase with decreasing density, increasing molecular weight, and intramolecular flexibility. The absolute value of $\hat{C}(0)$ is a measure of the strength of the intermolecular correlations and is a strongly increasing (decreasing) function of packing fraction (degree of polymerization).

The qualitative behavior of the structure factor at small wave vectors is controlled by a competition between intramolecular fluctuations and intermolecular correlations.

At the very smallest wave vectors, $kR_g < 1$, where R_g is the radius of gyration, one can expand the structure factor through second order about $k = 0$. Since the result is well-known, we simply state the result: the structure factor always *decreases* initially for inverse wave vectors larger than the radius of gyration. However, in the more experimentally interesting "intermediate" (universal) wave vector regime, $R_g^{-1} \ll k < \sigma^{-1}$, the intramolecular structure factor assumes the Debye scaling form: $\hat{\omega}(k) \sim 12(k\sigma)^{-2}$. Substituting this into eq 1c and expanding the Fourier transform of the direct correlation function through quadratic order, one obtains a Lorentzian form

$$\hat{S}(k) = \frac{1}{(k\sigma)^2 \theta + a^2} \quad (3a)$$

where

$$\theta \equiv 1 - \frac{1}{2} \sigma^{-2} \rho_m \hat{C}''(0); \quad a^2 \equiv -\rho_m \hat{C}(0) \quad (3b)$$

Two qualitatively different types of behavior are possible depending on the sign of θ . At sufficiently low densities and/or large chain lengths θ is positive, yielding a simple Lorentzian decay. Such "diffusive" behavior is analogous to the structure factor in the semidilute regime studied by Edwards⁵ and implies a screened Coulomb (Yukawa) decay of the total density fluctuations in real space with a screening length, ξ , given by

$$\xi = \sigma a^{-1} \theta^{1/2} \quad (4)$$

In the large N limit $a^2 \rightarrow 1/\hat{S}(0)$, and hence the screening length becomes proportional to the square root of the compressibility, which is a direct measure of the equilibrium density fluctuations. In particular, the density dependence of ξ in the liquid regime is significantly stronger²⁻⁴ than the $\rho_m^{-1/2}$ found for semidilute solutions.⁵ The second type of behavior can occur at sufficiently high density and/or low molecular weight where $\theta < 0$ whence eq 3a is valid only for $k\sigma \ll -a/\theta^{1/2}$. In this case the structure factor is a (weakly) increasing function of wave vector in the intermediate regime and therefore qualitatively resembles the simple atomic liquid case.⁸ A crossover between these two different behaviors is expected for particular values of density and molecular weight.

B. Numerical Results. In this subsection we present our numerical results for the structure factor of nono-

[†]This work performed at Sandia National Laboratories, supported by the U.S. Department of Energy under Contract DE-AC04-76DP00789.

[‡]The present paper is a continuation of the preceding paper in this issue¹ (referred to as paper 1) and prior publications²⁻⁴ and includes the wave vector dependent density fluctuations of polymer melts composed of nonoverlapping freely jointed chains.

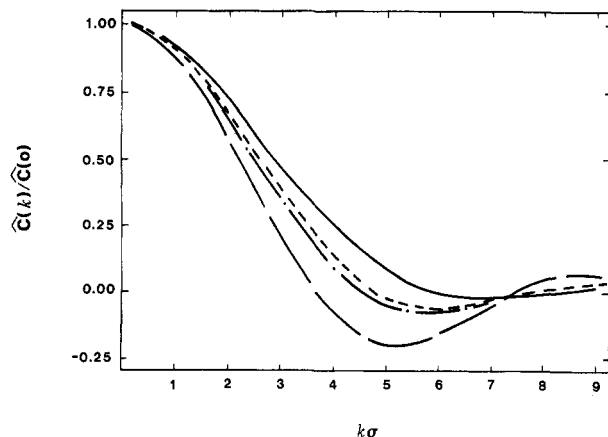


Figure 1. Fourier transform of the direct correlation function normalized by its zero wave vector value. Results are shown for the nonoverlapping freely jointed chain: $N = 2000$, $\eta_m = 0.5$, $\rho_m \hat{C}(0) = -1.445$ (short dash); $N = 2000$, $\eta_m = 0.3$, $\rho_m \hat{C}(0) = 0.13$ (long dash); $N = 20$, $\eta_m = 0.5$, $\rho_m \hat{C}(0) = -3.226$ (solid). The dash-dot curve is for the ideal freely jointed chain with $N = 2000$, $\eta_m = 0.5$, $\rho_m \hat{C}(0) = -2.1605$.

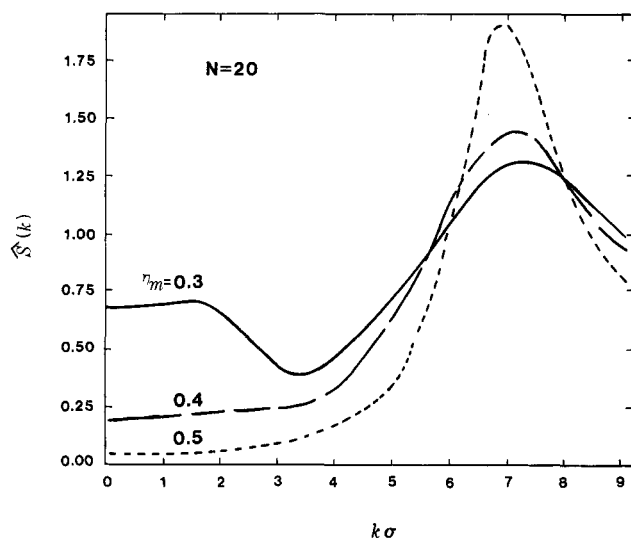


Figure 2. Structure factor of an $N = 20$ nonoverlapping freely jointed chain melt at three packing fractions.

verlapping freely jointed chains for a variety of packing fractions and degrees of polymerization. It is worth reemphasizing that we consider only the "tangent" bead-rod models in which the intramolecular bond length and hard-sphere diameter are equal. More general bead-rod models are straightforwardly treated.

The structure factors for $N = 20$ chains at three packing fractions are presented in Figure 2. The small wave vector regime is very sensitive to density both in magnitude and functional form.⁹ In particular, at $\eta_m = 0.3$, $\hat{S}(k)$ initially increases slightly and then goes through a minimum at $k\sigma \approx 3.5$ corresponding to the intramolecular excluded volume effect on $\hat{\omega}(k)$ (see Figure 1 of paper 1). As the density increases, long wavelength density fluctuations are strongly suppressed and the structure factor rises monotonically. The peak at high wave vectors is compound in nature reflecting both the fixed bond length constraint and local intermolecular structure in the melt. The high wave vector peak increases in intensity and decreases in position as the system densifies. More specifically, $\hat{\omega}(k)$ attains a local maximum of ≈ 1.276 at $k\sigma \approx 7.6$, while the maximum $\rho_m \hat{h}(k)$ is 0.096 (0.703) at $k\sigma \approx 6.4$ (6.9) for $\eta_m = 0.3$ (0.5).

The results of an analogous set of calculations for $N = 2000$ are shown in Figure 3a. The enhanced screening present in the high polymer melt results in significantly

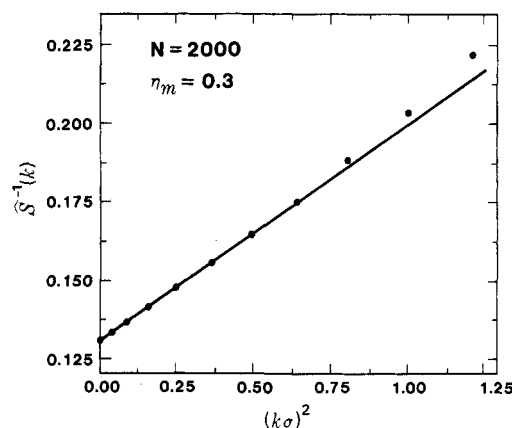
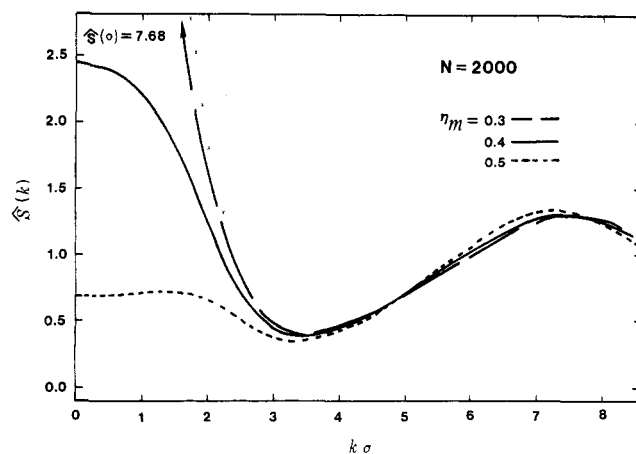


Figure 3. (a, Top) Same as Figure 2 but for $N = 2000$. The $\eta_m = 0.3$ curve goes off scale and attains the indicated value at $k = 0$. The small crosses represent the corresponding intramolecular structure factor, $\hat{\omega}(k)$, and beyond $k\sigma \approx 2.5$ it is indistinguishable on the scale of the plot from the full $\eta_m = 0.3$ structure factor. (b, Bottom) Ornstein-Zernike plot of the inverse structure factor versus the dimensionless wave vector squared in the intermediate regime. The solid circles are the RISM results, and the line is a fit through the small wave vector points.

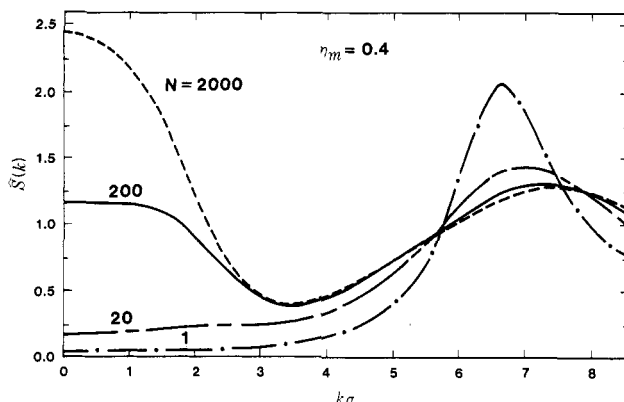


Figure 4. Structure factor of nonoverlapping freely jointed chain melt at fixed packing fraction for three values of degree of polymerization. The atomic hard-sphere Percus-Yevick result is also plotted.

different small wave vector behavior. In particular, the relatively smaller degree of intermolecular order produces diffusivelike behavior on long length scales. Indeed, for $\eta_m = 0.3$ the structure factor is very nearly Lorentzian, as demonstrated in Figure 3b, even though the polymer density is roughly 130 times greater than the semidilute crossover concentration.

A direct comparison of the N dependence of the structure factor at fixed packing fraction is presented in Figure

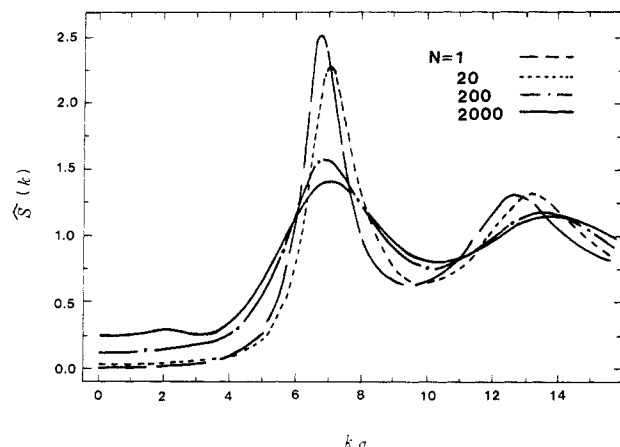


Figure 5. Same as Figure 4 but for N -dependent packing fractions chosen to mimic the polymethylene experimental values (see text): $\eta_m = 0.549$ for $N = 20$, $\eta_m = 0.571$ for $N = 200$, and $\eta_m = 0.572$ for $N = 2000$. The Percus-Yevick hard-sphere result for $\eta_m = 0.45$ is also shown.

4. Note the crossover from semidiluteline behavior at small wave vectors to simple liquidlike behavior with decreasing N . The Percus-Yevick result⁸ for atomic hard spheres is also plotted for comparison. Figure 4 is a vivid demonstration of the complementary relationship between bulk density and degree of polymerization resulting from the significant screening effects in polymer melts composed of flexible, ideal chains.

An attempt to make contact with real systems is presented in Figure 5 where the structure factor for $N = 20$, 200, and 2000 freely jointed chain melts with packing fractions representative of alkane liquids is plotted. The packing fractions employed are identical with those used in Figure 8 of paper 1. Clearly, the N dependence of $\hat{S}(k)$ seen in Figure 5 is much less than that in Figure 4, especially at small wave vectors, but there remain significant differences at high wave vectors reflecting the different short-range order (see Figure 9 in paper 1).

The effect of intramolecular overlap on the computed structure factor has been explored by comparing ideal freely jointed chains with their nonoverlapping counterparts. Although we do not plot the results here, the general features of $\hat{S}(k)$ and trends with N and η_m are qualitatively similar. Indeed, the structure factor appears to be considerably less sensitive to intramolecular structure details than the radial distribution function (see Figure 7 of paper 1). This is a consequence of a partial compensation effect between $\hat{\omega}(k)$ and $\hat{h}(k)$ arising from the general fact that the intermolecular structure is a functional of the intramolecular correlations.

Finally, the zero wave vector limit of the structure factor is related to the isothermal compressibility, κ_T via

$$\hat{S}(0) = \rho_m k_B T \kappa_T \quad (5)$$

The molecular weight dependence of this quantity for ideal and nonoverlapping freely jointed chains is plotted in Figure 6 for two high-density states. The relative differences between the ideal and nonoverlapping cases are qualitatively similar to the behavior of $g(\sigma^+)$ (see Figure 10 of paper 1). In addition, as found for $g(\sigma^+)$, convergence to a limiting value is slow, especially for the nonoverlapping chain, but it appears to be considerably more rapid at the higher density.

There are two important questions concerning our results in this section: (1) How reliable are the RISM predictions, especially for high N and small wave vectors? (2) What are the experimental implications of these results?

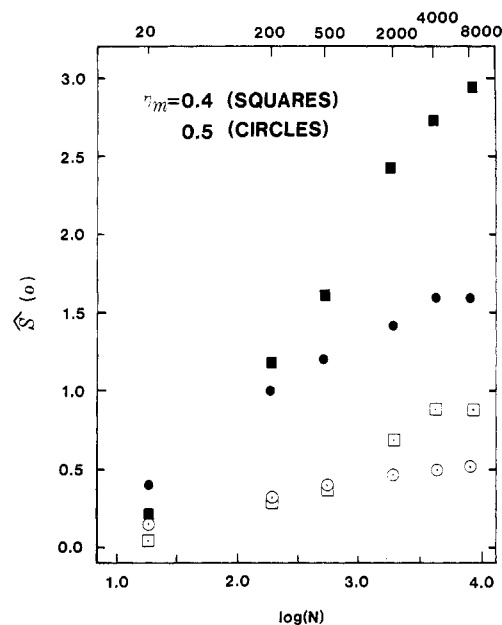


Figure 6. Zero wave vector limit of the structure factor of nonoverlapping (solid squares and circles) and ideal (open square and circles) freely jointed chain melts as a function of the logarithm of the degree of polymerization and two values of the packing fraction. The corresponding values of N are listed along the top horizontal axis.

Concerning the first question, it is hard to come to an a priori conclusion since even for small rigid molecules $\hat{S}(k)$ is difficult to reliably compute at small wave vectors via molecular dynamics or Monte Carlo computer simulation.¹¹ This occurs since $\hat{S}(0)$ requires $\hat{h}(0)$, and such a long-wavelength property is sensitive to numerical uncertainties. For flexible polymers, as discussed in paper 1, we believe that RISM is quite accurate for local structure. In addition, on long length scales and large N the integral equation theory reduces (see section III.A) to the correct limiting form for the correlation hole as predicted by deGennes.⁷ Nevertheless, there are indications that RISM overestimates the magnitude of small wave vector density fluctuations, especially for long chains. This conclusion is based on our comparison of the virial and compressibility equation of state predictions,¹⁰ which imply that the $\hat{S}(0)$ computed via RISM is being overestimated by approximately a factor of 2–3. A full discussion of these issues is presented elsewhere,¹⁰ but we simply note here that even for small, rigid molecules RISM tends to overestimate the zero wave vector compressibility, and this behavior is presumably related to known deficiencies of RISM on large length scales.^{12,13} In addition, neglect of the self-consistency issues discussed in paper 1 can be increasingly serious as the molecular weight increases. The magnitude of such deficiencies in the case of high polymers and specific properties remains to be quantified and fully understood, but their existence does not automatically imply that the local intermolecular structure predicted by RISM is in serious error. There are several recent studies¹⁴ which document the fact that integral equation theories that have difficulties describing certain long-wavelength properties nevertheless represent an accurate and reliable tool for studying short-range order.

Turning to the second question raised above, we first note that the crossover in the small wave vector form of $\hat{S}(k)$ from “diffusive” to small-molecule-like behavior predicted by RISM must be qualitatively correct. This conclusion follows immediately from the general and rigorous analysis represented in section II.A. The only

question is how accurately, for the specific model of choice, does RISM predict the quantitative point of the crossovers as a function of density and degree of polymerization. From eq 3b, one sees that the crossover is controlled by the curvature of the direct correlation function at zero wave vector, *not* by $\hat{C}(0)$ itself. Therefore, it is conceivable that even if $\hat{S}(0)$ is being overestimated by our formulation of RISM for polymers (implying an underestimate of $\hat{C}(0)$, (see eq 4)) $\theta(\rho_m, N)$ may be more accurately predicted, and hence the shape of $\hat{S}(k)$ at small k could be more reliable. Finally, we note that in regards to *real* systems the predicted crossover phenomenon may be a moot point since the relevant packing fractions of high polymer melts are very large (see paper 1). Therefore, a "diffusive" $\hat{S}(k)$ may be hard to observe experimentally, unless the degree of polymerization is *very* high ($N > 10^4$) or the polymer liquid can be significantly diluted by either elevated temperature or possibly the preparation of a *very* concentrated solution ($C \sim 100C^*$).

Our final comments concern the limitations and implications of our numerical results and model, especially with regard to the slow convergence with N . Clearly, a more experimentally sensible way to study the degree of polymerization dependence of observables is comparison at *constant pressure*, not at fixed packing fraction. Such a program has been carried out by us utilizing the RISM theory to determine the virial equation of state.¹⁰ Fixing the pressure induces a significant N dependence of the density (as found experimentally) which severely suppresses any large N dependence of properties such as the compressibility, static structure factor, and pair correlation function.¹⁰ Another point, discussed at length in paper 1, is that for highly flexible models, such as the freely jointed chain, corrections introduced by a fully self-consistent treatment of intramolecular and intermolecular correlations may be significant. In particular, we expect such corrections to be larger for the more compressible melts composed of longer chains, and the net result would again be a suppression of the N dependence of observables even at fixed packing fraction. Finally, as the level of chemical detail included in the intramolecular model is raised (e.g., wormlike chain), the chains become stiffer and are able to pack more efficiently. The introduction of a relatively short length scale (e.g., persistence length) associated with intramolecular stiffness will provide a natural mechanism for the development of sharper local order and, presumably, a concomitant suppression of a large sensitivity to the global length scale controlled by the degree of polymerization.

II. Comparison with the Predictions of Incompressible and Continuum Limit Models

A. Incompressible Limit. The incompressible random-phase approximation of deGennes⁷ assumes the vanishing of density fluctuations in neat polymer melts at *all* wave vectors: $\hat{S}(k) = 0$. It is therefore completely devoid of content for describing the neat polymer liquid structure factor. The connection between our RISM integral equation theory and the incompressible RPA for the *partial* (site-site) structure factors has been derived elsewhere.⁴ The incompressibility condition does make a specific prediction for the intermolecular pair correlation function given by^{3,7}

$$\rho_m h(r) = -\omega(r) \quad (6)$$

This prediction is universal in the sense that the deviation from the bulk density of monomers on different chains around a tagged site is independent of density and intermolecular forces.

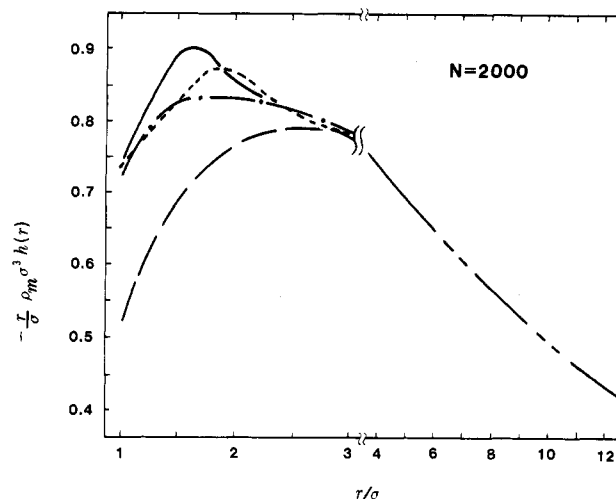


Figure 7. Total intermolecular correlation function times reduced density and separation for a high molecular weight model and several intramolecular models: Gaussian chain, $\eta_m = 0.5$ (short-dash) and $\eta_m = 0.3$ (dash-dot); ideal freely-jointed chain, $\eta_m = 0.4$ (solid); nonoverlapping freely jointed chain, $\eta_m = 0.3$ (long dash). Note the break in the horizontal axis between $r/\sigma = 3$ and 4. Beyond $r/\sigma \approx 4$ all four curves fall on the same curve (long dash-two short dashes) to within the resolution of the figure.

Equation 6 can be deduced from the generalized Ornstein-Zernike formalism by making a specific limiting assumption. In particular, we have the general result

$$\rho_m \hat{h}(k) = \rho_m \hat{\omega}^2(k) \hat{C}(k) [1 - \rho_m \hat{C}(k) \hat{\omega}(k)]^{-1} \quad (7)$$

If one makes the assumption

$$-\rho_m \hat{\omega}(k) \hat{C}(k) \gg 1 \quad (8)$$

then eq 7 reduces to the incompressible prediction of eq 6. Since $\hat{C}(k) \rightarrow 0$ for large k (see Figure 1), eq 8 and hence eq 6, are valid only at relatively small wave vectors (large intermonomer separations) and large N , as expected, and in this regime eq 6 and 8 become more accurate with increasing density.

The purpose of this subsection is to test the ability of the incompressible model to describe our microscopic integral equation results and to establish the former's range of validity and applicability. We consider Gaussian chains and ideal and nonoverlapping freely jointed chains of high molecular weight ($N = 2000$). The packing fractions considered are deliberately chosen such that there is *no* structure in $g(r)$; i.e., $g(r)$ rises monotonically with increasing separation to its asymptotic value of unity. Such cases would seem to be optimum for the applicability of the simple incompressible model. Figure 7 presents our results for $-\rho_m h(r)$ (in dimensionless units) where the prefactor r has been included since it represents the inverse of the $N \rightarrow \infty$ limiting Coulomb behavior of $h(r)$ for large separations.⁷ There are two features of importance in Figure 7. First, at relatively small separations, $r \lesssim 3\sigma$, both specific system dependence (intramolecular models) and density dependence are evident. For both the ideal chain cases and the relatively low-density nonideal case, the initial rise of $rh(r)$ away from its contact value ($r \lesssim 2\sigma$) is exponential. Clearly, universal behavior does not apply, and the specific functional dependence of eq 6 is not valid even though all the $g(r)$ values calculated by RISM are smooth and monotonically increasing functions. The second feature, however, is that beyond $r \approx 4\sigma$ universal behavior is found to be an excellent approximation even for the freely jointed chain with intramolecular excluded volume, and the specific form of $h(r)$ is in good agreement with eq 6. The latter result is in accord with our previous

findings³ for Gaussian ring polymers at relatively lower packing fractions than those considered in Figure 7. In addition, even for the very high density ($\eta_m = 0.5$) nonoverlapping freely jointed chain (not plotted in the figure) the behavior for $r \gtrsim 4\sigma$ also falls very nearly on the same curve! This occurs despite the fact that a modest amount of short-range structure is present for this system (see Figure 4a in paper 1).

In conclusion, the simple incompressibility relation appears to be remarkably accurate for flexible high molecular weight polymer liquids at relatively "large" separations, $r \gtrsim 4\sigma$; hence they provide an accurate description of the long-range intermolecular correlations in dense melts. However, at "small" separations, $r \lesssim 4\sigma$, the incompressible description fails even for ideal polymers, which display no sharp intermolecular structural features.

B. $N \rightarrow \infty$ Continuum Limit Model. A great deal of recent theoretical work has concentrated on deriving "scaling laws" valid in the $N \rightarrow \infty$ limit which are independent of the details of local chemical structure.⁷ Such studies often adopt an Edwards-like description^{5,6} of polymer structure in which the finite range intramolecular and intermolecular hard-core repulsions are replaced by δ -function pseudopotentials. The latter approximation corresponds in our language to letting the microscopic hard-core diameter approach zero with a finite value for the reduced monomer density $\rho_m \sigma^3$ and a divergence of the radius of gyration in the melt. We refer to such a model as the "continuum limit model".

Our interest in such a limiting model resides in what it predicts for the intermolecular pair correlation function within the generalized Ornstein-Zernike/RISM formalism. The major simplification introduced by the continuum limit is that the scaling or intermediate wave vector regime, defined as $R_g^{-1} \ll k < \sigma^{-1}$, plays a dominant role, and the simplifications of the intermediate regime previously invoked (see section II.A) can be introduced in the general equation for $\hat{h}(k)$ (see eq 7) and can be assumed to be valid for *all* wave vectors. Substituting $\hat{\omega}(k) = 12(k\sigma)^{-2}$ and $\hat{C}(k) = \hat{C}(0) \equiv C_0$ (which follows from the assumed δ -function repulsion) into eq 7, one obtains

$$\rho_m \hat{h}(K) = \frac{144}{K^2} \frac{\rho_m C_0}{K^2 - 12\rho_m C_0} \quad (9)$$

where $K \equiv r/\sigma$. Equation 9 can be Fourier inverted analytically. The result is

$$\rho_m \sigma^3 h(R) = \frac{-3}{\pi R} + \frac{3}{\pi R} e^{-R/\xi} \quad (10)$$

where $R \equiv r/\sigma$ and the dimensionless screening length is

$$\xi^{-1} = [-12\rho_m C_0]^{1/2} = (\hat{S}(0)/12)^{1/2} \quad (11)$$

The result in eq 10 contains two fundamentally different contributions: the first term is the universal asymptotic "correlation hole" contribution derived by deGennes⁷ based on incompressibility and describes the long-range intermolecular correlations induced by polymeric connectivity. The second term is system and density specific and describes the local short-range correlations that decay via density fluctuations in the fluid. The general form of eq 10 can be interpreted as suggesting that in general the intermolecular pair correlations in polymer melts contain two fundamentally distinct physical contributions: a universal long-range correlation and a small molecule, liquidlike short-range order. In the continuum limit model these two aspects can be rigorously separated. For realistic finite size monomer and molecular weight cases, a complete separation cannot be rigorously made, but our results in Figure 7 suggest such a decomposition approximately holds

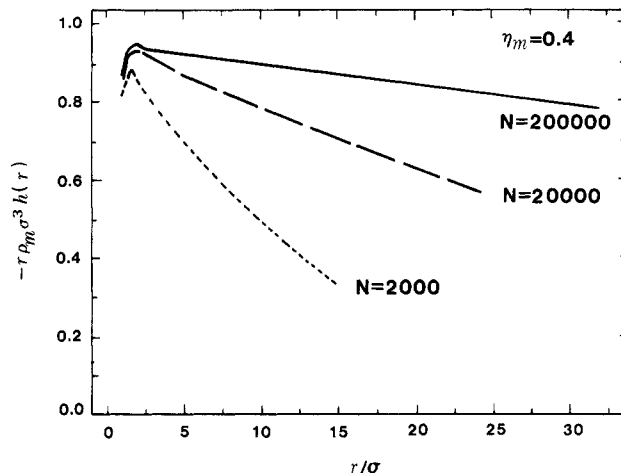


Figure 8. Same as Figure 7 but for three Gaussian chains of very high molecular weight at a fixed packing fraction. Each curve is plotted out to the value of r/σ where $g(r/\sigma) = 0.98$. The corresponding radii of gyration are $R_g/\sigma = 18.26$ ($N = 2000$), 57.735 ($N = 20000$), and 182.6 ($N = 200000$).

for flexible high molecular weight polymers.

Within the continuum model the direct correlation parameter, $\hat{C}(0) = C_0$ (which is the dense liquid analogue of the δ -function pseudopotential strength in polymer solutions), can be self-consistently determined by invoking the "core" condition: $h(r=0) = -1$ (implying the contact value $g(\sigma^+) = 0$). Employing eq 10 and 11 and performing the integral, one obtains the simple result

$$\xi = 3/(\pi(\rho_m \sigma^3)) \quad (12)$$

The inverse relation between liquid density and screening length is stronger, as expected, than the $\xi \sim \rho_m^{-1/2}$ result derived by Edwards for semidilute solutions.^{5,6} However, it is weaker than the results found from numerical solution of the RISM equations for large Gaussian chains⁴ with a nonzero hard-core diameter, which obey roughly $\xi \sim \rho_m^{-2}$ over the dense liquid regime. In addition, the absolute magnitude of ξ/σ for the continuum model is roughly a factor of 2–3 times smaller than its full RISM counterpart. Both these trends are typical of continuum models, which neglect the finite size of molecular subunits.¹⁵

Finally, we note that an *approximate* result for $h(r)$ of the form in eq 10 can be derived for melts composed of monomers of finite size. As before, in the intermediate wave vector regime $\hat{\omega}(k) \sim 12(k\sigma)^{-2}$ and $\hat{C}(k)$ can be represented as a quadratic function of $k\sigma$ (see Figure 1). If one *assumes* the resulting expression for $\hat{h}(k)$ is valid for all k , then the inverse Fourier transform can be interpreted as approximately describing the real space intermediate regime $\sigma < r \ll R_g$. Mathematically, a result identical in form with eq 10 is obtained except $\exp(-R/\xi) \rightarrow \theta^{-1} \times \exp(-R/\xi)$ and $\xi^{-2} = -12\rho_m C_0/\theta$, where θ is defined in eq 3b. The validity and limitations of such a simple analytic description can be tested by plotting $-\rho_m \sigma^3 h(r)$ calculated by RISM versus r/σ . If a continuum-like description applies, then the former quantity should be constant over the regime $\sigma < r \ll R_g$ and exponential for r/σ near unity. Numerical results for a series of *very* high molecular weight athermal Gaussian chains at a fixed packing fraction are plotted in Figure 8. At very small separations, exponential behavior is found, but significant corrections to Coulomb-like scaling on intermediate length scales are clearly evident.

III. Summary and Discussion

The present paper has had two major objectives. The first was to study in detail the static structure factor of

nonoverlapping athermal freely jointed chain melts over the entire wave vector regime. At zero wave vector we found that the compressibility was a strongly increasing (decreasing) function of degree of polymerization (density). The former trend reflects the enhanced self-screening and loss of intermolecular order with increasing N . The qualitative behavior of intermediate wave vectors is also very sensitive to N and packing fraction. Either "diffusive" semidilute-like behavior or simple liquid behavior is possible with a crossover region occurring for specific ranges of degree of polymerization and density. At large wave vectors, $\hat{S}(k)$ attains a local maximum which increases in magnitude and decreases in $k\sigma$ position and breadth as molecular weight (density) is decreased (increased). The peak is compound in nature, reflecting both the intramolecular bonding constraint and local intermolecular order. More general polymer models in which the chemical bond lengths and hard-sphere diameters are not equal will potentially allow a resolution of the intra- and intermolecular features. Finally, calculations performed for experimentally realistic, very highly packing fractions, at constant pressure,¹⁰ reveal a major suppression of molecular weight dependence of the structure factor.

Our second major theme was to contrast our microscopic RISM integral equation results with the predictions of simpler "more universal" theories. We found that the incompressible model was seriously inadequate at small intermolecular separations, even for high molecular weight systems which did not display any obvious structural features. This finding has potentially important consequences for the theoretical treatment of many polymer phenomena. For example, triplet exciton transport, or singlet exciton transfer via short-range exchange in polymeric systems with a high density of chromophores (e.g., polystyrene), is sensitive to local structure and may not be adequately described by theories which employ Gaussian configurational statistics and the incompressible model. However, beyond three to four monomer diameters, the incompressible model predictions are in excellent agreement with our high molecular weight RISM calculations, implying long-range correlations in dense polymer melts possess a high degree of universality even at finite N . On the other hand, we found very slow convergence to the $N \rightarrow \infty$ continuum limit predictions in the intermediate length scale regime, casting doubt on the quantitative usefulness of such a model for experimentally accessible molecular weights.

Many questions and theoretical directions remain to be pursued. An obvious one is the calculation of thermodynamic properties. A detailed study of the equation of state of athermal chains has been completed¹⁰ and reveals several interesting and surprising trends not accounted for

by simple lattice/mean field theories. Another technical direction is to further raise the level of chemical realism in our description of intramolecular structure. In particular, future work on homopolymer melts will focus on semiflexible wormlike chains and rotational isomeric-state chains. On a conceptual level, the construction of a fully self-consistent theory is being pursued. Such a development is important in potentially nonideal physical situations such as very high density/low-temperature homopolymer melts composed of stiff chains and certain polymer blends and block copolymer liquids. It may also be important for an accurate theoretical determination of the molecular weight dependence of local chain expansion. Self-consistency corrections will in general have both structural and thermodynamic consequences. A tractable generalization of our integral equation theory to blends¹⁶ and copolymers (alternating, random, and block)¹⁷ has been completed and provides microscopic expressions for the apparent Flory χ -parameter measured by neutron scattering. Finally, upon completion of the above theoretical program a host of important polymer phenomena will become amenable for the first time to a fully microscopic treatment, including phase separation and wide-angle X-ray scattering.

References and Notes

- (1) Schweizer, K. S.; Curro, J. G. *Macromolecules*, preceding paper in this issue.
- (2) Schweizer, K. S.; Curro, J. G. *Phys. Rev. Lett.* **1987**, *58*, 246.
- (3) Curro, J. G.; Schweizer, K. S. *Macromolecules* **1987**, *20*, 1928.
- (4) Curro, J. G.; Schweizer, K. S. *J. Chem. Phys.* **1987**, *87*, 1842.
- (5) Edwards, S. F. *Proc. Phys. Soc., London* **1966**, *88*, 265.
- (6) Doi, M.; Edwards, S. F. *The Theory of Polymer Dynamics*; Clarendon: Oxford, 1986.
- (7) deGennes, P.-G. *Scaling Concepts in Polymer Physics*; Cornell University: Ithaca, NY, 1979.
- (8) Hansen, J. P.; McDonald, I. R. *Theory of Simple Liquids*; Academic: London, 1976.
- (9) As we noted in section IIA, the structure factor initially decreases away from $k = 0$ for $kR_g < 1$. However, this regime is generally confined to very small values of $k\sigma$ for high polymers. Hence, in all our plots we do not plot the $kR_g < 1$ behavior but rather draw smooth curves from $\hat{S}(0)$ through the intermediate wave vector regime values.
- (10) Schweizer, K. S.; Curro, J. G. *J. Chem. Phys.*, in press.
- (11) Street, W. B.; Tildesley, D. J. *Faraday Discuss. Chem. Soc.* **1978**, No. 66, 27.
- (12) Topol, R.; Claverie, P. *Mol. Phys.* **1978**, *35*, 1753. Street, W. B.; Tildesley, P. J. *J. Chem. Phys.* **1978**, *68*, 1275.
- (13) Chandler, D. *Faraday Discuss. Chem. Soc.* **1978**, No. 66, 71. Sullivan, D. E.; Gray, C. G. *Mol. Phys.* **1981**, *42*, 443. Chandler, D.; Richardson, D. M. *J. Phys. Chem.* **1983**, *87*, 2060.
- (14) Rossky, P. J.; Pettit, B. M.; Stell, G. *Mol. Phys.* **1983**, *50*, 1263.
- (15) See, for example: Schweizer, K. S. *J. Chem. Phys.* **1986**, *85*, 4638.
- (16) Schweizer, K. S.; Curro, J. G. *Phys. Rev. Lett.* **1988**, *60*, 809. Curro, J. G.; Schweizer, K. S. *J. Chem. Phys.* **1988**, *88*, 7242.
- (17) Schweizer, K. S.; Curro, J. G., to be submitted for publication.